NCALD Antisense Oligonucleotide Therapy in Addition to Nusinersen further Ameliorates Spinal Muscular Atrophy in Mice

Laura Torres-Benito,[1,2,7] Svenja Schneider,[1,2,7] Roman Rombo,[1,2] Karen K. Ling,[3] Vanessa Grysko,[1,2] Aaradhita Upadhyay,[1,2] Natalia L. Kononenko,[4] Frank Rigo,[3] C. Frank Bennett,[3] and Brunhilde Wirth[1,2,5,6,*]

Spinal muscular atrophy (SMA) is a neuromuscular disease causing the most frequent genetic childhood lethality. Recently, nusinersen, an antisense oligonucleotide (ASO) that corrects *SMN2* splicing and thereby increases full-length SMN protein, has been approved by the FDA and EMA for SMA therapy. However, the administration of nusinersen in severe and/or post-symptomatic SMA-affected individuals is insufficient to counteract the disease. Therefore, additional SMN-independent therapies are needed to support the function of motoneurons and neuromuscular junctions. We recently identified asymptomatic *SMN1*-deleted individuals who were protected against SMA by reduced expression of neurocalcin delta (*NCALD*). NCALD reduction is proven to be a protective modifier of SMA across species, including worm, zebrafish, and mice. Here, we identified *Ncald*-ASO3—out of 450 developed *Ncald* ASOs—as the most efficient and non-toxic ASO for the CNS, by applying a stepwise screening strategy in cortical neurons and adult and neonatal mice. In a randomized-blinded preclinical study, a single subcutaneous low-dose *SMN*-ASO and a single intracerebroventricular *Ncald*-ASO3 or control-ASO injection were presymptomatically administered in a severe SMA mouse model. NCALD reduction of >70% persisted for about 1 month. While low-dose *SMN*-ASO rescues multiorgan impairment, additional NCALD reduction significantly ameliorated SMA pathology including electrophysiological and histological properties of neuromuscular junctions and muscle at P21 and motoric deficits at 3 months. The present study shows the additional benefit of a combinatorial SMN-dependent and SMN-independent ASO-based therapy for SMA. This work illustrates how a modifying gene, identified in some asymptomatic individuals, helps to develop a therapy for all SMA-affected individuals.

Spinal muscular atrophy (SMA) is an autosomal-recessive neurodegenerative disease characterized by the loss of α-motoneurons in the anterior horns of the spinal cord causing symmetrical muscle weakness and atrophy of limb and trunk muscles. SMA affects 1 in 6,000—10,000 live births and is the leading genetic cause of infant mortality.[1,2] In the European population 1:35 and worldwide 1:51 individuals are SMA carriers.[3,4] SMA is caused by deletions or loss-of-function mutations of *survival of motor neuron 1* (*SMN1* [MIM: 600354]) and a variable number of mainly non-functional *SMN2* copies resulting in low levels of the survival motor neuron (SMN) protein.[5,6] While *SMN1* produces only full-length (FL)-*SMN1* transcripts and protein, *SMN2* (MIM: 601627) mainly produces alternatively spliced transcripts (*SMN2Δ7*), which generate a truncated and unstable SMNΔ7 protein. Only a small amount of *SMN2* transcripts (~10%) are correctly spliced and are of full length, generating an SMN protein identical to the one produced from *SMN1* copies.[7,8] There is an inverse correlation between the number of *SMN2* copies and the severity of the disease. It can range from type I (SMA1 [MIM: 253300]), which represents the severe end of the spectrum and accounts for approximately 60% of 5q-SMA-affected individuals, to type IV, the mildest and adult form.[1,2,4,9] SMN is crucial for all cells, but abnormal low levels of SMN mainly affect spinal motoneurons innervating proximal muscles.[10]

Recently, nusinersen, the first antisense oligonucleotide (ASO)-based therapy for SMA-affected individuals, has been approved by the US Food & Drug Administration (FDA) and the European Medicines Agency (EMA).[11] Nusinersen is an *SMN*-ASO that increases SMN levels by blocking an intronic splice silencer in *SMN2*, thereby facilitating the exon 7 inclusion and generation of FL-*SMN2* transcripts.[12] Clinical studies in all types of SMA-affected individuals treated with nusinersen showed significant amelioration in motoric abilities in about half of them.[13,14] However, the therapeutic increment of SMN through the ASO approach seems to be insufficient to fully counteract the SMA pathology.[13,14] Despite encouraging on-going studies, it might be that even presymptomatic therapy with nusinersen is unable to provide sufficient SMN protein support for motoneuron function and thus stop disease progression over the patient's life-time in individuals with only one or two *SMN2* copies. Moreover, results from different animal models have shown a critical "therapeutic time window" in SMA, as increasing SMN postsymptomatically either

[1]Institute of Human Genetics, University of Cologne, 50931 Cologne, Germany; [2]Center for Molecular Medicine Cologne, University of Cologne, 50931 Cologne, Germany; [3]Ionis Pharmaceuticals, Carlsbad, CA 92008, USA; [4]Excellence Cluster on Cellular Stress Responses in Aging Associated Diseases (CECAD), University of Cologne, 50931 Cologne, Germany; [5]Institute for Genetics, University of Cologne, 50674 Cologne, Germany; [6]Center for Rare Diseases, University Hospital of Cologne, 50931 Cologne, Germany
[7]These authors contributed equally to this work
*Correspondence: brunhilde.wirth@uk-koeln.de
https://doi.org/10.1016/j.ajhg.2019.05.008.

fails or shows only a modest amelioration of symptoms in mice.[15–20] Similarly, in *SMN1*-deleted individuals, the highest effects were observed when early or presymptomatic therapeutic intervention was applied.[13,14] Since only few countries started to include *SMN1* deletion testing into the neonatal screening, in most instances SMA is detected only after the first clinical signs appear, which means that a large number of motoneurons are already affected; this fact drastically reduces the beneficial effect of any therapy. Therefore, the development of SMN-independent therapies can be beneficial (1) as an additional support of motoneurons and neuromuscular junction (NMJ) function under conditions when SMN elevation via SMN-dependent therapy is insufficient (e.g., ASO therapy in SMA-affected individuals with SMA1, who possess only one or two *SMN2* copies) and (2) after the disease onset in all SMA types, to support the function of motoneurons and NMJs in an SMN-independent manner.

The strongest support of a potential beneficial impact of SMN-independent therapeutic approaches originates from our knowledge gained on SMA-protective genetic modifiers in humans.[21,22] In asymptomatic *SMN1*-deleted individuals, we found two SMA-protective modifiers able to counteract the SMN deficiency and prevent the disease phenotype. In 2008, we identified the first human SMA genetic modifier, *Plastin 3* (*PLS3* [MIM: 300131]), and provided conclusive evidence that its overexpression exerts protective effects in *in vitro* and *in vivo* SMA models.[21,23–25] Further studies using AAV9-PLS3 in SMA mice strengthened our findings.[26] In 2017, we reported a second SMA-protective modifier gene, *Neurocalcin delta* (*NCALD* [MIM: 606722]).[22] We found that reduced levels of NCALD, which is a neuronal Ca^{2+} sensor protein, acts protective in a four-generation discordant family with five asymptomatic and two SMA1-affected individuals. Multiple *in vitro* and *in vivo* experiments have shown that reducing NCALD levels significantly ameliorate SMA pathology across SMA species.[22] Most importantly, heterozygous *Ncald* knockout in a severely affected SMA mouse model (SMA-*Ncald*$^{ko/wt}$) injected with a low dose *SMN*-ASO (30 μg) at P1 to rescue multiorgan dysfunction ameliorates the neuromuscular pathology including motor axon development, both NMJ size and maturation, muscle size, proprioceptive input on motoneuron soma, as well as endocytic uptake of FM1-43 dye at the NMJ and motoric abilities.[22] Moreover, heterozygous in contrast to homozygous *Ncald* knockout has no effect on brain development and adult neurogenesis, but enhances spinal motor neuron development.[27] Collectively, these results demonstrate that genetically mediated NCALD reduction acts beneficially on SMA pathology.

Based on these encouraging results, we (1) developed and analyzed specific *Ncald*-ASOs to efficiently downregulate NCALD in mouse spinal cord and (2) used them in a randomized and blinded preclinical study in the severely affected SMA mouse model in a combination with low-dose SMN splice switching ASOs. This is a proof of concept for a combinatorial SMN-dependent and SMN-independent ASO-based therapy in SMA mice.

To study *in vivo* the effect of NCALD downregulation and evaluate its effect on SMA pathology, we first had to develop a non-toxic and efficient ASO. Therefore, we designed 450 different 2′-O-methoxyethyl (MOE)-gapmer *Ncald* ASOs on mixed backbone, which were first tested in cultured embryonic mouse cortical neurons for downregulation of *Ncald* mRNA using a quantitative RT-PCR assay. A subset of 22 hits from the cell culture screen, mainly targeting the 3′ UTR of *Ncald* RNA, were further tested in adult mice for tolerability and efficiency (Figure 1A). Adult mice were treated by intracerebroventricular (i.c.v.) bolus injection with 500 μg of each ASO. Two weeks later, *Ncald* expression was verified in spinal cord and brain lysates by qRT-PCR (Figure 1B). None of the ASOs overlapped with the primer probe set (PPS) which were flanking exon 5–6 junction; therefore, amplicon effect of oligonucleotides was not a concern (Figure S1A). Since the Taiwanese SMA mice (who carry two human *SMN2* copies per allele and no functional murine *Smn* gene) on C57BL6/N background survive around 2 weeks[23,28] and the best clinical outcome is expected in a presymptomatic therapy, the three most efficient *Ncald*-ASOs (Ionis #673672, #673663, #673756; further referred as *Ncald*-ASO1, -ASO2, or -ASO3, respectively) or a control ASO (Ionis #676626, Ctrl-ASO) were tested in neonatal mice (Figures S1B and S1C). To evaluate the tolerability and efficiency and to determine the optimal dose in these young animals, i.c.v. injections with different doses, ranging from 30 to 60 μg of *Ncald*-ASO1, -ASO2, -ASO3, and Ctrl-ASO were carried out at postnatal day 2 (P2). At P10 we examined NCALD downregulation in spinal cord and brain lysates of mice injected with *Ncald*-ASOs in comparison to Ctrl-ASO-injected mice. We found that i.c.v. delivery of *Ncald*-ASO1 and *Ncald*-ASO2 showed acute toxicity, since 30% and 50% of the injected animals died (data not shown); Ctrl-ASO and *Ncald*-ASO3 were well tolerated by all animals. Since mice treated with 30 to 60 μg of *Ncald*-ASO3 exhibited only a moderate downregulation of NCALD (Figure S2), we increased the dose to 100 μg and obtained an 80% and 75% NCALD downregulation in the spinal cord and the brain, respectively (Figure 1C). Therefore, 100 μg of *Ncald*-ASO3 was applied for the whole study.

All our experiments were carried out in the Taiwanese severe SMA mouse model on a mixed$_{50}$ background (50% FVB/N: 50% C57BL6/N), which is slightly more robust than congenic FVB/N or C57BL6/N mice; SMA mice on mixed$_{50}$ background die at 16.5 days.[22–24] By applying our previously developed breeding scheme (Figure 2),[29] 50% of mice develop SMA (*Smn*$^{ko/ko}$;*SMN2*$^{tg/0}$) and 50% are healthy SMA carriers (*Smn*$^{ko/wt}$;*SMN2*$^{tg/0}$, defined as heterozygous [HET] and used as controls). Since our previous studies showed that none of the genetic modifiers (PLS3, NCALD, or CHP1) are able to rescue the severe SMA phenotype,[22–24,30] we pharmacologically elevated the SMN levels—mainly in the non-central nervous system

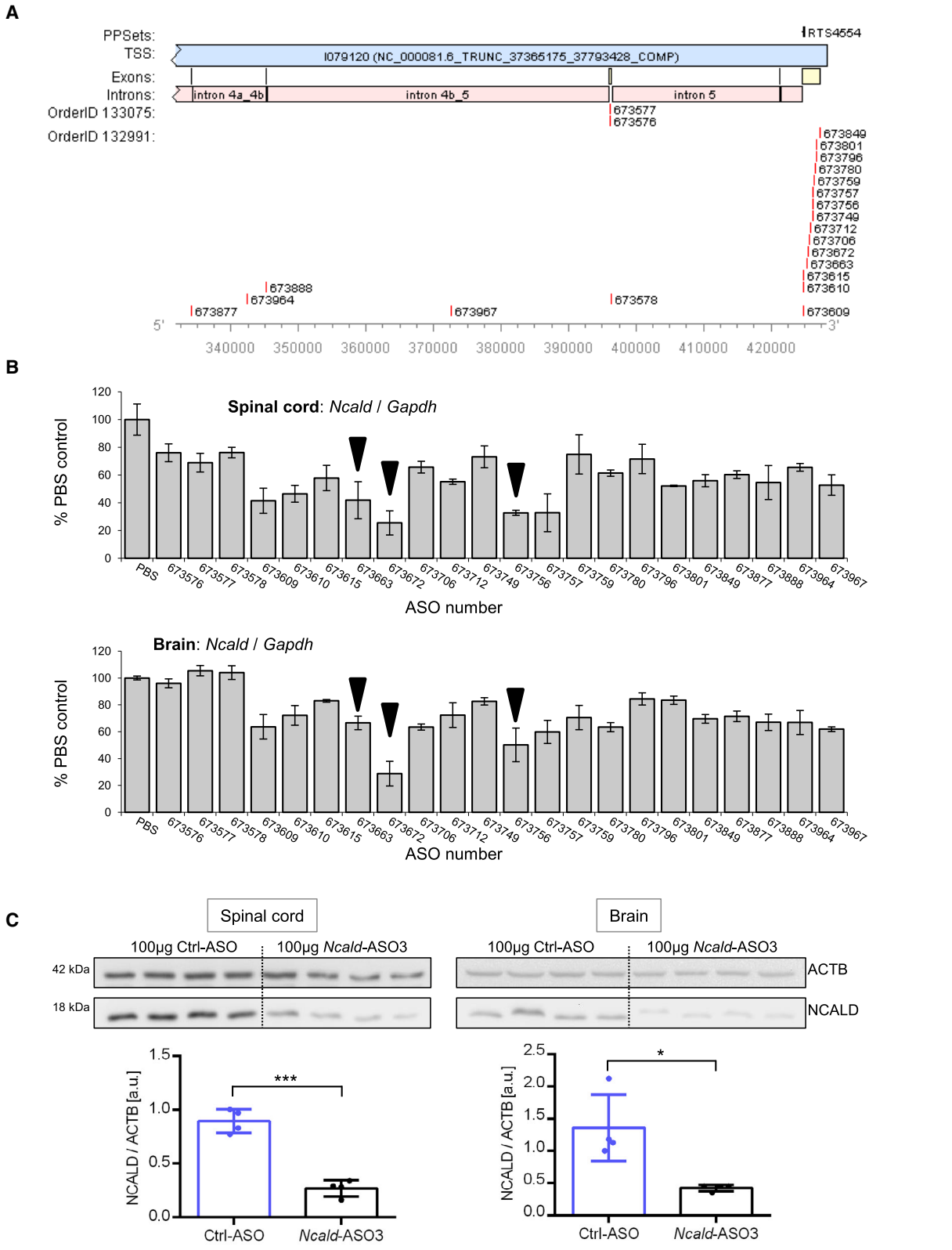

Figure 1. Target Regions of Tested *Ncald*-ASOs and Knockdown Efficiency in Spinal Cord and Brain of Adult Wild-Type Mice
(A) Numbers of generated *Ncald*-ASOs and their respective target site in the mouse *Ncald* gene are shown. Used reference sequence is the *Mus musculus* strain C57BL/6J chromosome 15, GRCm38.p4 C57BL/6J (GenBank: NC_000081.6). Exons are labeled in yellow, introns in pink.

(legend continued on next page)

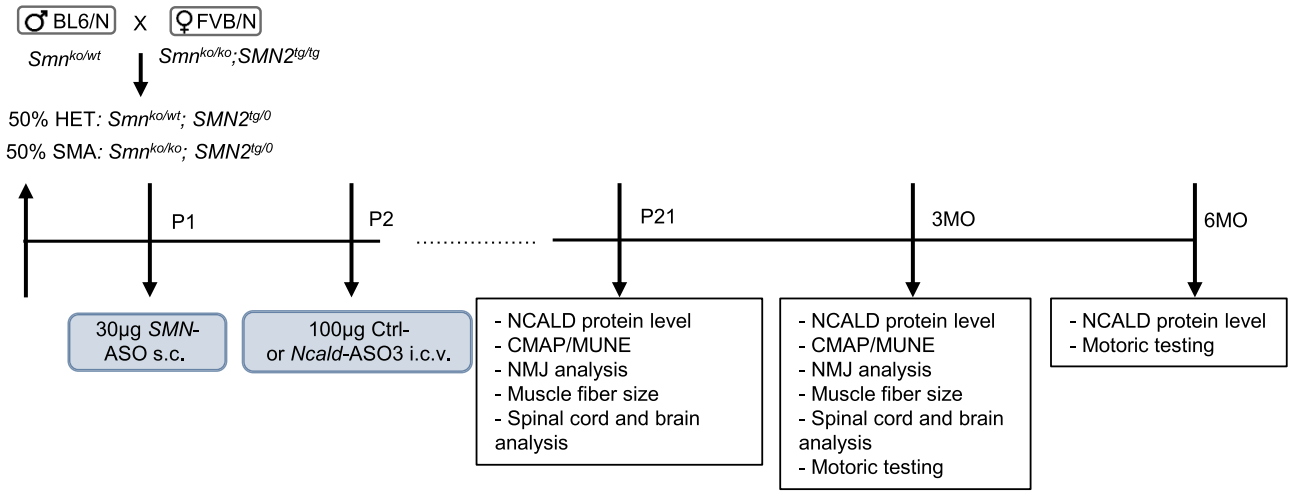

Figure 2. Experimental Design and Time Points of Individual Analyses
A graph showing the breeding scheme to obtain severe SMA and HET mice on mixed$_{50}$ background (upper left), ASO treatments (blue boxes), and individual analyses at the indicated time points P21 and 3 and 6 months (MO). s.c., subcutaneous; i.c.v., intracerebroventricular; CMAP, compound muscle action potential; MUNE, motor unit number estimation; NMJ, neuromuscular junction.

organs—by applying subcutaneously a single low dose of the SMN splice switching ASO (*SMN*-ASO, nusinersen). Therefore, all animals were subcutaneously injected with 30 µg of *SMN*-ASO at P1 (Figure 2A). We confirmed our previous results, showing that systemic injection of low-dose *SMN*-ASO has a major impact on survival, while the mice still show all SMA typical deficits (reduced compound muscle action potential [CMAP] and motor unit estimation [MUNE], impaired NMJ and muscle structure, reduced motoric abilities). Note also, we avoided a high dose of SMN-ASO since this provides a full rescue of SMA in mice,[31] making the analysis of the effect of the *Ncald* ASO impossible. Thus, the low-dose nusinersen-treated SMA model resembles a mild SMA phenotype, similar to an SMA-affected individual carrying 3–4 *SMN2* copies or the genotype found in our asymptomatic individuals or an SMA1-affected individual treated with nusinersen.[32,33]

To better evaluate the requirement of NCALD from birth to adult age and beyond, we first determined endogenous NCALD level in spinal cord and brain of HET and SMA mice (injected with 30 µg *SMN*-ASO at P1) at P4, P21, 6, and 10 months. Our data show that NCALD is particularly abundant in spinal cord at very early developmental stages and gradually decreases when NMJs starts to develop and mature and muscles became more and more active. This is in line with our former finding that NCALD suppresses clathrin-mediated endocytosis, a process highly required for synaptic vesicle recycling at the NMJ.[22] In contrast, NCALD level in the brain increases at P21 and stays high throughout the adulthood, although it slightly decreases at 10 months (Figure S3); this is in line with its important role in adult neurogenesis.[27]

We next analyzed the efficiency of *Ncald*-ASO3 in spinal cord and brain. We obtained four different study groups originated from litters treated with *Ncald*-ASO3 (referred to as SMA *Ncald*-ASO3 and HET *Ncald*-ASO3 mice) and from litters injected with Ctrl-ASO (referred to as SMA Ctrl-ASO and HET Ctrl-ASO mice). Mice were sacrificed at P21 and 3 months to examine the efficiency of the *Ncald*-ASO3 in spinal cord and brain. At P21, the NCALD amount was significantly reduced in both SMA and HET mice treated with *Ncald*-ASO3 in comparison to Ctrl-injected mice (Figure 3A). However, no differences were observed at 3 months between *Ncald*- and Ctrl-ASO-treated mice (Figure 3B), suggesting that the *Ncald*-ASO3 effect persists for about 1 month and reaches Ctrl-ASO levels by 3 months. Importantly, the postnatal *Ncald*-ASO3 treatment has no effect on brain morphology, which is in line with our previous data from heterozygous *Ncald* knockout mice[27] (Figure S4).

Since *Ncald*-ASO3 efficiently reduced NCALD levels in spinal cord at P21, we investigated the impact on main SMA-affected cell types, motoneurons and muscles, and studied neuromuscular circuitry and muscle strength by applying four independent approaches: (1) electrophysiological measurements, i.e., compound muscle action potential (CMAP) and motor unit estimation (MUNE), (2) immunostaining of histological sections to analyze

(B) The 22 most efficient *Ncald*-ASOs were applied in adult wild-type mice by intracerebroventricular (i.c.v.) bolus injection and knockdown efficiency was determined by qRT-PCR of *Ncald* (primer probe set flanks exon 5–6 junction) relative to *Gapdh* (control) expression in spinal cord and brain. *Ncald*-ASOs marked by black triangle were tested in neonatal mice.
(C) NCALD protein levels in the spinal cord and the brain of P10 animals (n = 4 animals per genotype) treated i.c.v. at P2 with 100 µg *Ncald*-ASO3 were more than 70% reduced compared to mice injected with 100 µg of Ctrl-ASO. Numbers on the left indicate respective band size in kDa. ACTB, loading control. Unpaired, two-tailed Student's t test; *$p < 0.05$, ***$p < 0.001$.

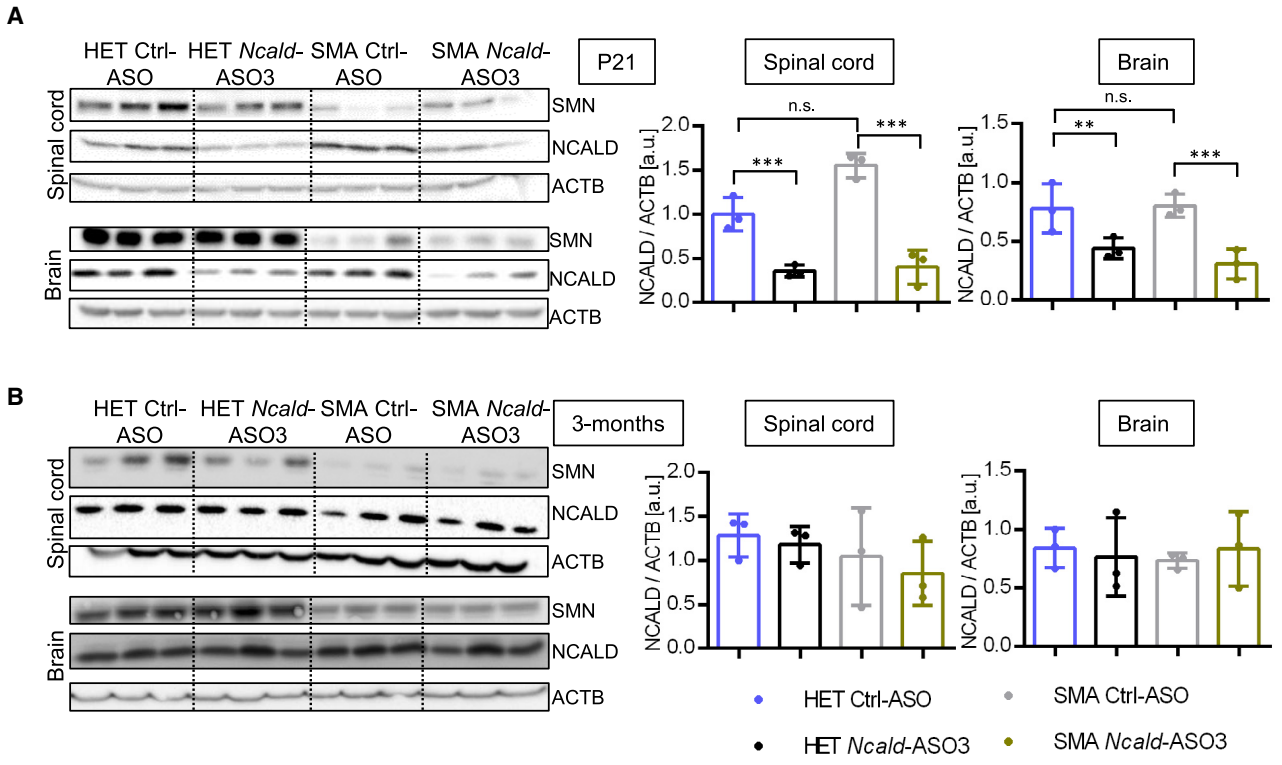

Figure 3. Temporal Progression of NCALD Protein Levels in Mice Injected with *SMN*-ASO at P1 and Ctrl-ASO or *Ncald*-ASO3 at P2
Western blot analysis of NCALD and SMN levels in the spinal cord and the brain at (A) P21 and (B) 3 months after injection with respective ASOs (n = 3 per genotype and age). NCALD protein levels normalized to ACTB (loading control) are shown on the right side. NCALD levels are significantly decreased in both spinal cord and brain of HET and SMA animals co-injected with *SMN*-ASO and *Ncald*-ASO3 at P21 (A) but not at 3 months (B). Color legend for graphs is displayed at the bottom. For statistics, ordinary one-way ANOVA was applied with Tukey posthoc test for multiple comparisons; n.s., not significant, $^{**}p < 0.01$, $^{***}p < 0.001$.

neuromuscular junction (NMJ) size and maturity, (3) determination of muscle fiber size, and (4) examination of muscle force using the grip strength test.

First, we analyzed animals at P21, when NCALD was visibly reduced to >70%; moreover, this is a time point when NMJs are fully matured and functional in mice. Second, we analyzed the animals at 3 months. Although NCALD was no longer reduced upon a single injection, we speculated whether the effect on motoneuron development and function could be beneficial even at a later time point.

At P21, CMAP and MUNE, both known to be excellent predictors of muscle-nerve functionality at the NMJ, were performed. Both are well documented to be reduced in SMA mouse models and SMA individuals.[19,34,35] CMAP represents the maximal response of a given muscle upon the stimulation of the efferent nerve, and MUNE gives information about the number of motor units that innervate a muscle or a group of muscles.[36] The electrophysiological assays were performed in the gastrocnemius muscle. SMA Ctrl-ASO-treated mice exhibited highly decreased CMAP amplitude and MUNE in comparison with HET Ctrl-ASO-treated animals, which upon NCALD reduction was significantly ameliorated in SMA mice (Figure 4A).

To verify whether improved CMAP and MUNE are due to an increase in NMJ size and maturity, we next analyzed the NMJ architecture in the *Transversus abdominis* (TVA) muscle, which is a well-known vulnerable muscle in SMA.[37] To discriminate NMJs individually, we stained the postsynaptic terminal with bungarotoxin, which reveals the distribution of the acetylcholine receptors (AChRs) and thus allows a determination of the size of the NMJ, and co-stained the presynaptic part with an antibody against neurofilament (Figure 4B). The area occupied by the AChRs in NMJs of SMA Ctrl-ASO-treated mice was reduced compared to HET Ctrl-ASO-treated mice. NCALD downregulation enhanced the amount of AChRs in SMA *Ncald*-ASO3-treated mice (Figure 4B). Moreover, NMJ maturity (defined as mature when ≥3 perforations and immature when <3 perforations are present[19]) was delayed in SMA Ctrl-ASO-compared to HET Ctrl-ASO-treated mice at P21, but rescued in SMA *Ncald*-ASO3-treated mice (Figure 4B).

Next, we assessed the effect of NCALD downregulation on muscle morphology by quantifying the diameter of gastrocnemius muscle fibers using transverse H&E-stained sections (Figure 4C). Muscle fibers were significantly smaller in SMA Ctrl-ASO mice compared to HET Ctrl-ASO-treated mice at P21. Upon NCALD downregulation, we observed that the mean size of the muscle fibers was

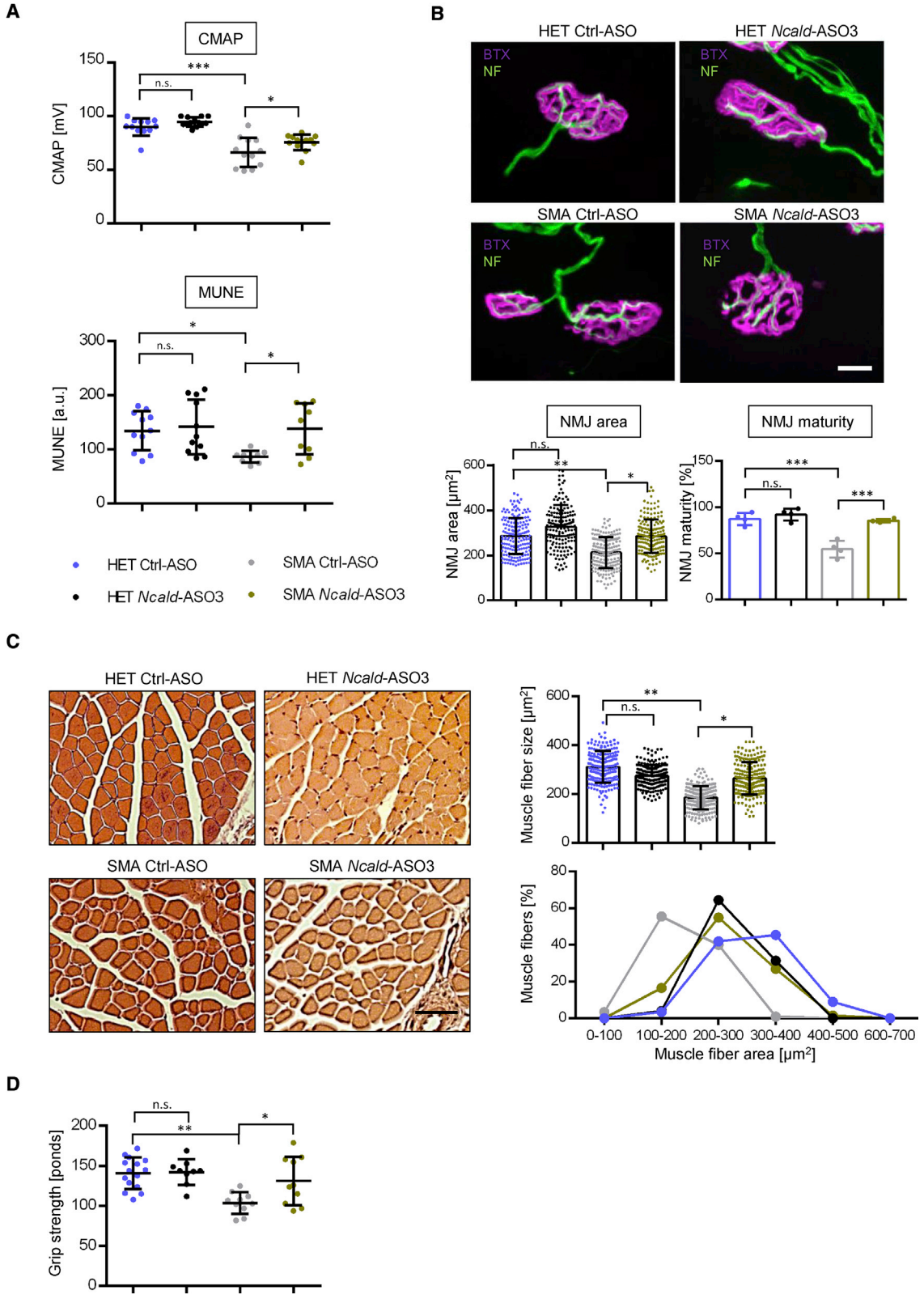

Figure 4. Electrophysiological, Structural, and Motoric Analysis of Mice Injected with *SMN*-ASO at P1 and Ctrl-ASO or *Ncald*-ASO3 at P2

(A) Dot plots of CMAP and MUNE values at P21 in HET and SMA mice with mean ± SD. Animals used for CMAP: HET Ctrl-ASO n = 12; HET *Ncald*-ASO3 n = 13; SMA Ctrl-ASO n = 12; SMA *Ncald*-ASO3 n = 13. MUNE: HET Ctrl-ASO n = 11; HET *Ncald*-ASO3 n = 11; SMA Ctrl-ASO n = 9; SMA *Ncald*-ASO3 n = 9.

(B) Representative NMJ images in HET and SMA animals at P21 showing postsynaptic NMJ region stained with bungarotoxin (BTX, magenta) and presynaptic nerve with neurofilament (NF, green). Scale bar: 10 µm. Graphs below the images show single dot plot values

(legend continued on next page)

rescued in SMA mice (Figure 4C). A detailed analysis of size-grouped fibers showed that the number of fibers with larger diameter, ranging from 200 to 400 μm, was significantly higher in SMA *Ncald*-ASO3 compared to SMA Ctrl-ASO mice (Figure 4C). These results suggest that NCALD downregulation in the nervous system of SMA mice ameliorates also muscle pathology.

Although the effect of a single injection of the *Ncald*-ASO3 at P2 was abolished at 3 months, we analyzed CMAP and MUNE at that age to ascertain whether the effect of early NCALD reduction that markedly restored motoneuron and muscle function to HET level could have a long-lasting effect and still improve the NMJ functionality and motor abilities. While SMA Ctrl-ASO-treated mice showed diminished CMAP amplitude and MUNE compared to HET Ctrl-ASO-treated mice, *Ncald*-ASO3 treatment had no positive effect on the electrophysiology biomarkers at 3 months (Figure S5A). While the area occupied by the AChRs in NMJs of SMA Ctrl-ASO-treated mice was reduced compared to HET Ctrl-ASO-treated mice, the early NCALD downregulation had no long-term effect on NMJ area (Figure S5B). Lastly, while the muscle fiber size was clearly decreased in SMA Ctrl-ASO-treated mice, it was not restored to HET Ctrl-ASO-treated level (Figure S5C). Strikingly, the number of fibers with larger diameter, ranging from 200 to 400 μm in SMA *Ncald*-ASO3-treated animals was similar to HET Ctrl-ASO-treated mice, suggesting a long-lasting effect of improved NMJs development and maturation under NCALD reduction on the muscle structure.

Lastly, to assess the motoric ability in these mice and to strengthen the electrophysiology and histological results, we performed a grip strength test with adult mice at 3 and 6 months.[22] At both ages, SMA Ctrl-ASO-treated mice displayed reduced grip strength in comparison with HET Ctrl-ASO-treated mice. Interestingly, 3-month-old SMA *Ncald*-ASO3-treated animals performed significantly better in the grip strength test compared to SMA Ctrl-ASO mice (Figure 4D), but not at 6 months (Figure S5D). These data demonstrate a beneficial effect of neonatal NCALD downregulation on motor performance until 3 months in SMA mice, which might be driven by the early improvement in NMJ structure and innervation as well as by the increase in muscle fiber size.

In summary, we developed a *Ncald*-ASO that highly efficiently downregulates NCALD protein levels by about 70% for about 1 month and is non-toxic for CNS development and maturation. Previously, we and others have shown that endocytosis is strongly decreased in SMA. Through multiple *in vitro* and *in vivo* experiments, we have demonstrated that NCALD reduction restores impaired endocytosis in SMA.[22] Thus, similar to the genetically induced NCALD reduction, a single i.c.v. injection of *Ncald* ASO3 reduces the NCALD amount especially during the most critical time of NMJ development and maturation and thus facilitates synaptic vesicles endocytosis and neurotransmission in SMA, which is severely affected.

Indeed, a single neonatal CNS injection of *Ncald*-ASO3 in a combinatorial therapy with a single low-dose SMN-ASO systemic injection improved all neuromuscular deficits in SMA mice including (1) electrophysiological properties (CMAP and MUNE) and thus NMJ neurotransmission, (2) NMJ area and maturity, and (3) muscle fiber size at P21. Furthermore, this beneficial effect of *Ncald*-ASO3 on the development and function of motoneurons and muscles has a long-lasting effect even 3 months later, when SMA *Ncald*-ASO3-treated mice show significantly increased motoric strength compared to SMA *Ctrl*-ASO-treated mice.

Since endogenous NCALD is gradually downregulated after P4 and reaches about 20%–25% at 10 months, it suggests that under physiological conditions, motoneurons downregulate NCALD levels postnatally to achieve the most efficient endocytic recycling of synaptic vesicles, required for proper NMJ function. Via *Ncald* ASO3 therapy, we achieve the facilitation of synaptic vesicle recycling earlier in the development, thus improving the neurotransmission and as a consequence the NMJ maturation and function in SMA.

While *SMN*-ASOs, small molecules, or *SMN* gene therapy show promising results in pre- or early-treated symptomatic SMA individuals, treatment in more advanced stages of the disease show only moderate or even no effect.[1,31,33,38,39] For these SMA-affected individuals, amelioration or even stopping the disease progression is crucial and therefore requires further SMN-dependent and SMN-independent therapies.[40,41] Moreover, the capacity of *SMN*-ASOs or small molecules to restore endogenous *SMN2* splicing is below 2-fold in spinal cord and brain, which is likely insufficient to counteract loss of SMN, especially in SMA1-affected individuals with only one or two *SMN2* copies, even if treated presymptomatically.[6,33,42–44] It has also been shown in SMA mice that SMN is mainly required before P17, corresponding to the period of NMJ development and maturation.[18]

Therefore, additional SMN-independent approaches allowing life-long maintenance of motoneurons and NMJ function are needed. The advantage of this system is that both genes (*SMN* and *NCALD*) will be targeted by the same system: an ASO approach. We accomplish NCALD

of NMJ areas of all grouped animals with mean ± SD and quantification of maturity of NMJs with mean values of mice per group ± SD. Statistics was performed with mean values of animals per group. n = 4 animals per group, 30–55 NMJs per animal.
(C) Representative pictures and quantifications of hematoxylin and eosin-stained gastrocnemius (GC) muscle fibers from HET and SMA animals at P21. Scale bar: 50 μm. Graphs on the right show single dot plot values of GC areas of all grouped animals with mean ± SD (n = 4 animals per genotype, n = 50 fibers/mouse). For visualization, muscle fibers were grouped according to the area intervals of 100 μm^2.
(D) Dot plot of grip strength in HET and SMA animals at 3 months. Single values of each animal are shown as mean ± SD. Number of animals used are: HET Ctrl-ASO n = 14, HET *Ncald*-ASO3 n = 9, SMA Ctrl-ASO n = 10, SMA *Ncald*-ASO3 n = 10.
Color legend for all graphs is displayed in (A). For all analyses, ordinary one-way ANOVA with Tukey posthoc test for multiple comparisons was applied. n.s., not significant, *$p < 0.05$, **$p < 0.01$, ***$p < 0.001$.

downregulation (more than 70% of protein levels) in the targeted tissues by a specific *Ncald*-ASO administration in P2 mice via i.c.v. injection. However, the *Ncald* MOE gapmer ASOs used to downregulate the RNA in comparison to the *SMN* MOE ASOs (nusinersen) that restores *SMN*2 splicing were less metabolically stable. While the *SMN*-ASOs are very stable upon subcutaneous injection and have a positive effect in liver even after 6 months,[31] the duration of the effect of the *Ncald*-ASO3 was highly efficient for about 1 month but disappeared after 3 months. This suggests that a monthly reinjection or further designs to optimize duration of action needs to be considered.

Our findings provide the proof of concept that NCALD-mediated ASO downregulation in CNS is possible and demonstrate that *Ncald*-ASO3 can ameliorate SMA pathology and motoric dysfunction upon a single presymptomatic injection in neonatal animals. Although NCALD protein and its repressor role is gradually downregulated in spinal cord from P4 to 10 months, it still could be that a repetitively monthly i.c.v. bolus injection of the *Ncald*-ASO3 in the first few months could further enhance the positive impact, resembling the effect of the genetically modified SMA-*Ncald*$^{ko/wt}$ mice.[22] A future perspective of the present study is to design ASOs against human NCALD and analyze the effect in cultured motoneurons derived from human iPSC, which then might be used to treat SMA-affected individuals. Finally, this work illustrates how a modifying gene uncovered in some asymptomatic individuals contributes to development of a therapy for all SMA-affected individuals.

Supplemental Data

Supplemental Data can be found online at https://doi.org/10.1016/j.ajhg.2019.05.008.

Acknowledgments

This study was support by DFG Wi945/17-1, RTG 1960, DFG Wi945/19-1, (B.W.), CMMC C16 (B.W.), DFG KO5091/2-1 (N.L.K.), SMA Europe (L.T.-B.), and Ottomar Päsel Stiftung (S.S.).

Declaration of interests

C.F.B., F.R., and K.K.L. are employees of IONIS Pharmaceuticals. B.W. holds US patent 9,988,626 B2 approved June 5, 2018, Neurocalcin Delta Inhibitors and Therapeutic and Non-Therapeutic Uses Thereof.

Received: April 12, 2019
Accepted: May 10, 2019
Published: June 20, 2019

References

1. Finkel, R.S., Mercuri, E., Meyer, O.H., Simonds, A.K., Schroth, M.K., Graham, R.J., Kirschner, J., Iannaccone, S.T., Crawford, T.O., Woods, S., et al.; SMA Care group (2018). Diagnosis and management of spinal muscular atrophy: Part 2: Pulmonary and acute care; medications, supplements and immunizations; other organ systems; and ethics. Neuromuscul. Disord. *28*, 197–207.
2. Mercuri, E., Finkel, R.S., Muntoni, F., Wirth, B., Montes, J., Main, M., Mazzone, E.S., Vitale, M., Snyder, B., Quijano-Roy, S., et al.; SMA Care Group (2018). Diagnosis and management of spinal muscular atrophy: Part 1: Recommendations for diagnosis, rehabilitation, orthopedic and nutritional care. Neuromuscul. Disord. *28*, 103–115.
3. Sugarman, E.A., Nagan, N., Zhu, H., Akmaev, V.R., Zhou, Z., Rohlfs, E.M., Flynn, K., Hendrickson, B.C., Scholl, T., Sirko-Osadsa, D.A., and Allitto, B.A. (2012). Pan-ethnic carrier screening and prenatal diagnosis for spinal muscular atrophy: clinical laboratory analysis of >72,400 specimens. Eur. J. Hum. Genet. *20*, 27–32.
4. Feldkötter, M., Schwarzer, V., Wirth, R., Wienker, T.F., and Wirth, B. (2002). Quantitative analyses of SMN1 and SMN2 based on real-time lightCycler PCR: fast and highly reliable carrier testing and prediction of severity of spinal muscular atrophy. Am. J. Hum. Genet. *70*, 358–368.
5. Lefebvre, S., Bürglen, L., Reboullet, S., Clermont, O., Burlet, P., Viollet, L., Benichou, B., Cruaud, C., Millasseau, P., Zeviani, M., et al. (1995). Identification and characterization of a spinal muscular atrophy-determining gene. Cell *80*, 155–165.
6. Wirth, B. (2000). An update of the mutation spectrum of the survival motor neuron gene (SMN1) in autosomal recessive spinal muscular atrophy (SMA). Hum. Mutat. *15*, 228–237.
7. Lorson, C.L., Hahnen, E., Androphy, E.J., and Wirth, B. (1999). A single nucleotide in the SMN gene regulates splicing and is responsible for spinal muscular atrophy. Proc. Natl. Acad. Sci. USA *96*, 6307–6311.
8. Lorson, C.L., Strasswimmer, J., Yao, J.M., Baleja, J.D., Hahnen, E., Wirth, B., Le, T., Burghes, A.H., and Androphy, E.J. (1998). SMN oligomerization defect correlates with spinal muscular atrophy severity. Nat. Genet. *19*, 63–66.
9. Wirth, B., Brichta, L., Schrank, B., Lochmüller, H., Blick, S., Baasner, A., and Heller, R. (2006). Mildly affected patients with spinal muscular atrophy are partially protected by an increased SMN2 copy number. Hum. Genet. *119*, 422–428.
10. Tisdale, S., and Pellizzoni, L. (2015). Disease mechanisms and therapeutic approaches in spinal muscular atrophy. J. Neurosci. *35*, 8691–8700.
11. Hoy, S.M. (2017). Nusinersen: First Global Approval. Drugs *77*, 473–479.
12. Rigo, F., Chun, S.J., Norris, D.A., Hung, G., Lee, S., Matson, J., Fey, R.A., Gaus, H., Hua, Y., Grundy, J.S., et al. (2014). Pharmacology of a central nervous system delivered 2′-O-methoxyethyl-modified survival of motor neuron splicing oligonucleotide in mice and nonhuman primates. J. Pharmacol. Exp. Ther. *350*, 46–55.
13. Finkel, R.S., Mercuri, E., Darras, B.T., Connolly, A.M., Kuntz, N.L., Kirschner, J., Chiriboga, C.A., Saito, K., Servais, L., Tizzano, E., et al.; ENDEAR Study Group (2017). Nusinersen versus Sham Control in Infantile-Onset Spinal Muscular Atrophy. N. Engl. J. Med. *377*, 1723–1732.
14. Mercuri, E., Darras, B.T., Chiriboga, C.A., Day, J.W., Campbell, C., Connolly, A.M., Iannaccone, S.T., Kirschner, J., Kuntz, N.L., Saito, K., et al.; CHERISH Study Group (2018). Nusinersen versus Sham Control in Later-Onset Spinal Muscular Atrophy. N. Engl. J. Med. *378*, 625–635.
15. Murray, L.M., Gillingwater, T.H., and Parson, S.H. (2010). Using mouse cranial muscles to investigate neuromuscular pathology in vivo. Neuromuscul. Disord. *20*, 740–743.

16. Lutz, C.M., Kariya, S., Patruni, S., Osborne, M.A., Liu, D., Henderson, C.E., Li, D.K., Pellizzoni, L., Rojas, J., Valenzuela, D.M., et al. (2011). Postsymptomatic restoration of SMN rescues the disease phenotype in a mouse model of severe spinal muscular atrophy. J. Clin. Invest. *121*, 3029–3041.
17. Robbins, K.L., Glascock, J.J., Osman, E.Y., Miller, M.R., and Lorson, C.L. (2014). Defining the therapeutic window in a severe animal model of spinal muscular atrophy. Hum. Mol. Genet. *23*, 4559–4568.
18. Kariya, S., Obis, T., Garone, C., Akay, T., Sera, F., Iwata, S., Homma, S., and Monani, U.R. (2014). Requirement of enhanced Survival Motoneuron protein imposed during neuromuscular junction maturation. J. Clin. Invest. *124*, 785–800.
19. Bogdanik, L.P., Osborne, M.A., Davis, C., Martin, W.P., Austin, A., Rigo, F., Bennett, C.F., and Lutz, C.M. (2015). Systemic, postsymptomatic antisense oligonucleotide rescues motor unit maturation delay in a new mouse model for type II/III spinal muscular atrophy. Proc. Natl. Acad. Sci. USA *112*, E5863–E5872.
20. Zhou, H., Meng, J., Marrosu, E., Janghra, N., Morgan, J., and Muntoni, F. (2015). Repeated low doses of morpholino antisense oligomer: an intermediate mouse model of spinal muscular atrophy to explore the window of therapeutic response. Hum. Mol. Genet. *24*, 6265–6277.
21. Oprea, G.E., Kröber, S., McWhorter, M.L., Rossoll, W., Müller, S., Krawczak, M., Bassell, G.J., Beattie, C.E., and Wirth, B. (2008). Plastin 3 is a protective modifier of autosomal recessive spinal muscular atrophy. Science *320*, 524–527.
22. Riessland, M., Kaczmarek, A., Schneider, S., Swoboda, K.J., Löhr, H., Bradler, C., Grysko, V., Dimitriadi, M., Hosseinibarkooie, S., Torres-Benito, L., et al. (2017). Neurocalcin Delta Suppression Protects against Spinal Muscular Atrophy in Humans and across Species by Restoring Impaired Endocytosis. Am. J. Hum. Genet. *100*, 297–315.
23. Ackermann, B., Kröber, S., Torres-Benito, L., Borgmann, A., Peters, M., Hosseini Barkooie, S.M., Tejero, R., Jakubik, M., Schreml, J., Milbradt, J., et al. (2013). Plastin 3 ameliorates spinal muscular atrophy via delayed axon pruning and improves neuromuscular junction functionality. Hum. Mol. Genet. *22*, 1328–1347.
24. Hosseinibarkooie, S., Peters, M., Torres-Benito, L., Rastetter, R.H., Hupperich, K., Hoffmann, A., Mendoza-Ferreira, N., Kaczmarek, A., Janzen, E., Milbradt, J., et al. (2016). The Power of Human Protective Modifiers: PLS3 and CORO1C Unravel Impaired Endocytosis in Spinal Muscular Atrophy and Rescue SMA Phenotype. Am. J. Hum. Genet. *99*, 647–665.
25. Heesen, L., Peitz, M., Torres-Benito, L., Hölker, I., Hupperich, K., Dobrindt, K., Jungverdorben, J., Ritzenhofen, S., Weykopf, B., Eckert, D., et al. (2016). Plastin 3 is upregulated in iPSC-derived motoneurons from asymptomatic SMN1-deleted individuals. Cell. Mol. Life Sci. *73*, 2089–2104.
26. Kaifer, K.A., Villalón, E., Osman, E.Y., Glascock, J.J., Arnold, L.L., Cornelison, D.D.W., and Lorson, C.L. (2017). Plastin-3 extends survival and reduces severity in mouse models of spinal muscular atrophy. JCI Insight *2*, e89970.
27. Upadhyay, A., Hosseinibarkooie, S., Schneider, S., Kaczmarek, A., Torres-Benito, L., Mendoza-Ferreira, N., Overhoff, M., Rombo, R., Grysko, V., Kye, M.J., et al. (2019). Neurocalcin Delta Knockout Impairs Adult Neurogenesis Whereas Half Reduction Is Not Pathological. Front. Mol. Neurosci. *12*, 19.
28. Hosseinibarkooie, S., Schneider, S., and Wirth, B. (2017). Advances in understanding the role of disease-associated proteins in spinal muscular atrophy. Expert Rev. Proteomics *14*, 581–592.
29. Riessland, M., Ackermann, B., Förster, A., Jakubik, M., Hauke, J., Garbes, L., Fritzsche, I., Mende, Y., Blumcke, I., Hahnen, E., and Wirth, B. (2010). SAHA ameliorates the SMA phenotype in two mouse models for spinal muscular atrophy. Hum. Mol. Genet. *19*, 1492–1506.
30. Janzen, E., Mendoza-Ferreira, N., Hosseinibarkooie, S., Schneider, S., Hupperich, K., Tschanz, T., Grysko, V., Riessland, M., Hammerschmidt, M., Rigo, F., et al. (2018). CHP1 reduction ameliorates spinal muscular atrophy pathology by restoring calcineurin activity and endocytosis. Brain *141*, 2343–2361.
31. Hua, Y., Sahashi, K., Rigo, F., Hung, G., Horev, G., Bennett, C.F., and Krainer, A.R. (2011). Peripheral SMN restoration is essential for long-term rescue of a severe spinal muscular atrophy mouse model. Nature *478*, 123–126.
32. Helmken, C., Hofmann, Y., Schoenen, F., Oprea, G., Raschke, H., Rudnik-Schöneborn, S., Zerres, K., and Wirth, B. (2003). Evidence for a modifying pathway in SMA discordant families: reduced SMN level decreases the amount of its interacting partners and Htra2-beta1. Hum. Genet. *114*, 11–21.
33. Finkel, R.S., Chiriboga, C.A., Vajsar, J., Day, J.W., Montes, J., De Vivo, D.C., Yamashita, M., Rigo, F., Hung, G., Schneider, E., et al. (2016). Treatment of infantile-onset spinal muscular atrophy with nusinersen: a phase 2, open-label, dose-escalation study. Lancet *388*, 3017–3026.
34. Arnold, W.D., Porensky, P.N., McGovern, V.L., Iyer, C.C., Duque, S., Li, X., Meyer, K., Schmelzer, L., Kaspar, B.K., Kolb, S.J., et al. (2014). Electrophysiological Biomarkers in Spinal Muscular Atrophy: Preclinical Proof of Concept. Ann. Clin. Transl. Neurol. *1*, 34–44.
35. Swoboda, K.J., Prior, T.W., Scott, C.B., McNaught, T.P., Wride, M.C., Reyna, S.P., and Bromberg, M.B. (2005). Natural history of denervation in SMA: relation to age, SMN2 copy number, and function. Ann. Neurol. *57*, 704–712.
36. Arnold, W.D., Sheth, K.A., Wier, C.G., Kissel, J.T., Burghes, A.H., and Kolb, S.J. (2015). Electrophysiological Motor Unit Number Estimation (MUNE) Measuring Compound Muscle Action Potential (CMAP) in Mouse Hindlimb Muscles. J. Vis. Exp. (103).
37. Murray, L.M., Lee, S., Bäumer, D., Parson, S.H., Talbot, K., and Gillingwater, T.H. (2010). Pre-symptomatic development of lower motor neuron connectivity in a mouse model of severe spinal muscular atrophy. Hum. Mol. Genet. *19*, 420–433.
38. Mendell, J.R., Al-Zaidy, S., Shell, R., Arnold, W.D., Rodino-Klapac, L.R., Prior, T.W., Lowes, L., Alfano, L., Berry, K., Church, K., et al. (2017). Single-Dose Gene-Replacement Therapy for Spinal Muscular Atrophy. N. Engl. J. Med. *377*, 1713–1722.
39. Naryshkin, N.A., Weetall, M., Dakka, A., Narasimhan, J., Zhao, X., Feng, Z., Ling, K.K., Karp, G.M., Qi, H., Woll, M.G., et al. (2014). Motor neuron disease. SMN2 splicing modifiers improve motor function and longevity in mice with spinal muscular atrophy. Science *345*, 688–693.
40. Wirth, B., Garbes, L., and Riessland, M. (2013). How genetic modifiers influence the phenotype of spinal muscular atrophy and suggest future therapeutic approaches. Curr. Opin. Genet. Dev. *23*, 330–338.
41. Talbot, K., and Tizzano, E.F. (2017). The clinical landscape for SMA in a new therapeutic era. Gene Ther. *24*, 529–533.

42. Poirier, A., Weetall, M., Heinig, K., Bucheli, F., Schoenlein, K., Alsenz, J., Bassett, S., Ullah, M., Senn, C., Ratni, H., et al. (2018). Risdiplam distributes and increases SMN protein in both the central nervous system and peripheral organs. Pharmacol. Res. Perspect. *6*, e00447.
43. Kletzl, H., Marquet, A., Günther, A., Tang, W., Heuberger, J., Groeneveld, G.J., Birkhoff, W., Mercuri, E., Lochmüller, H., Wood, C., et al. (2019). The oral splicing modifier RG7800 increases full length survival of motor neuron 2 mRNA and survival of motor neuron protein: Results from trials in healthy adults and patients with spinal muscular atrophy. Neuromuscul. Disord. *29*, 21–29.
44. Stevens, G., Yawitch, T., Rodda, J., Verhaart, S., and Krause, A. (1999). Different molecular basis for spinal muscular atrophy in South African black patients. Am. J. Med. Genet. *86*, 420–426.

The American Journal of Human Genetics, Volume *105*

Supplemental Data

NCALD Antisense Oligonucleotide Therapy in Addition to Nusinersen further Ameliorates Spinal Muscular Atrophy in Mice

Laura Torres-Benito, Svenja Schneider, Roman Rombo, Karen K. Ling, Vanessa Grysko, Aaradhita Upadhyay, Natalia L. Kononenko, Frank Rigo, C. Frank Bennett, and Brunhilde Wirth

SUPPLEMENTAL FIGURES AND LEGENDS

A

Ncald ex 5-6 PPS	Length (bp)	Sequence
***Ncald* ex 5-6P**	28	TCCGCCAGATGGATACCAATAGAGATGG
***Ncald* ex 5-6F**	21	TGCCTGAAGATGAATCAACCC
***Ncald* ex 5-6R**	19	AGGAGACGCACAATGGATG

B

IONIS #	Name	Chemistry	Results in neonatal injected mice
676626	Control-ASO	MOE-gapmer, mixed backbone	None of Control-ASO injected mice died
673672	*Ncald*-ASO1	MOE-gapmer, mixed backbone	30% of mice died after injection with *Ncald*-ASO1
673663	*Ncald*-ASO2	MOE-gapmer, mixed backbone	50% of mice died after injection with *Ncald*-ASO2
673756	*Ncald*-ASO3	MOE-gapmer, mixed backbone	None of *Ncald*-ASO3 injected mice died

C

IONIS #	Name	Length (bp)	Sequence
676626	Control-ASO	20	GTTTTCAAATACACCTTCAT
673672	*Ncald*-ASO1	20	AACACTTAATTTGGTCTGCA
673663	*Ncald*-ASO2	20	TGGCATTTGAATATGTGTTT
673756	*Ncald*-ASO3	20	GTGGTTCTTGTTTTACAGGA

Figure S1: ASO sequences, design and optimization.

(A) Prime probe sets used in the qRT-PCR to amplify mouse *Ncald* and evaluate downregulation in brain and spinal cord.

(B) Selected ASOs for neonatal injection and dosage optimization.

(C) Selected ASO sequences for neonatal injection and dosage optimization. bp = base pairs.

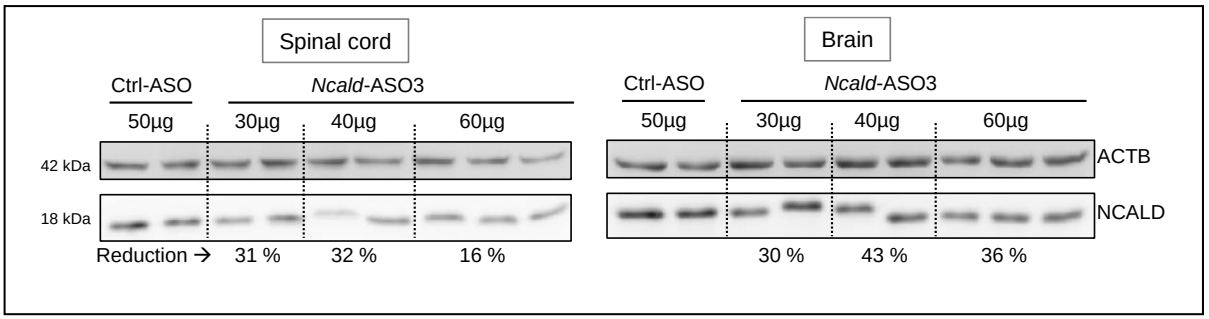

Figure S2: *Ncald*-ASO3 dosage optimization for i.c.v. injections in neonatal mice. Western blot analysis showing NCALD downregulation efficiency in the spinal cord and the brain of P10 *Ncald*-ASO3 HET and SMA animals intracerebroventicularly (i.c.v.) injected on postnatal day 2 (P2) with either 50 µg of Ctrl-ASO or 30, 40, or 60 µg of *Ncald*-ASO3. Numbers at the bottom indicate NCALD protein levels in *Ncald*-ASO3-treated animals normalized to the Ctrl-ASO injected animals in percentages. Numbers on the left indicate respective band size in kDa. ACTB = loading control. Unpaired, two-tailed Student´s *t*-test; * $P < 0.05$, *** $P < 0.001$.

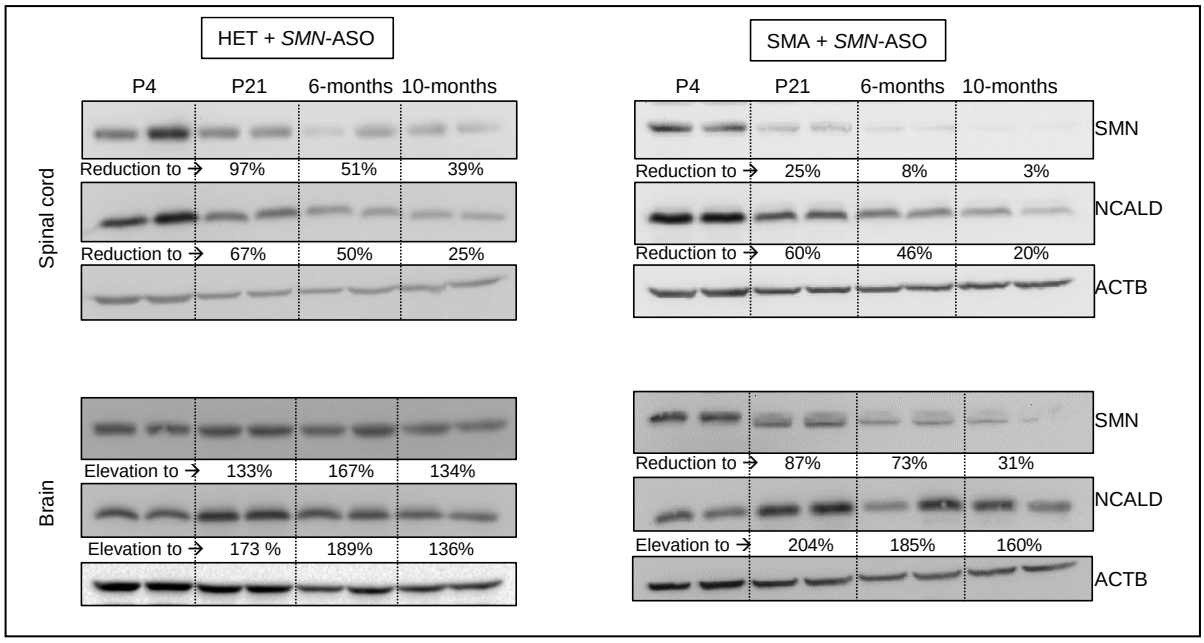

Figure S3: NCALD is naturally downregulated during adulthood in spinal cord.

Western blots of spinal cord and brain from HET and SMA animals injected with a single low-dose of 30 µg *SMN*-ASO: Spinal cord and brain samples were taken from mice at the indicated time points P4, P21, 6 months and 10 months to analyze the time course behavior of SMN and NCALD protein levels. Note that in contrary to the brain, NCALD levels in the spinal cord in both HET and SMA animals are decreasing during the adulthood. ACTB= loading control.

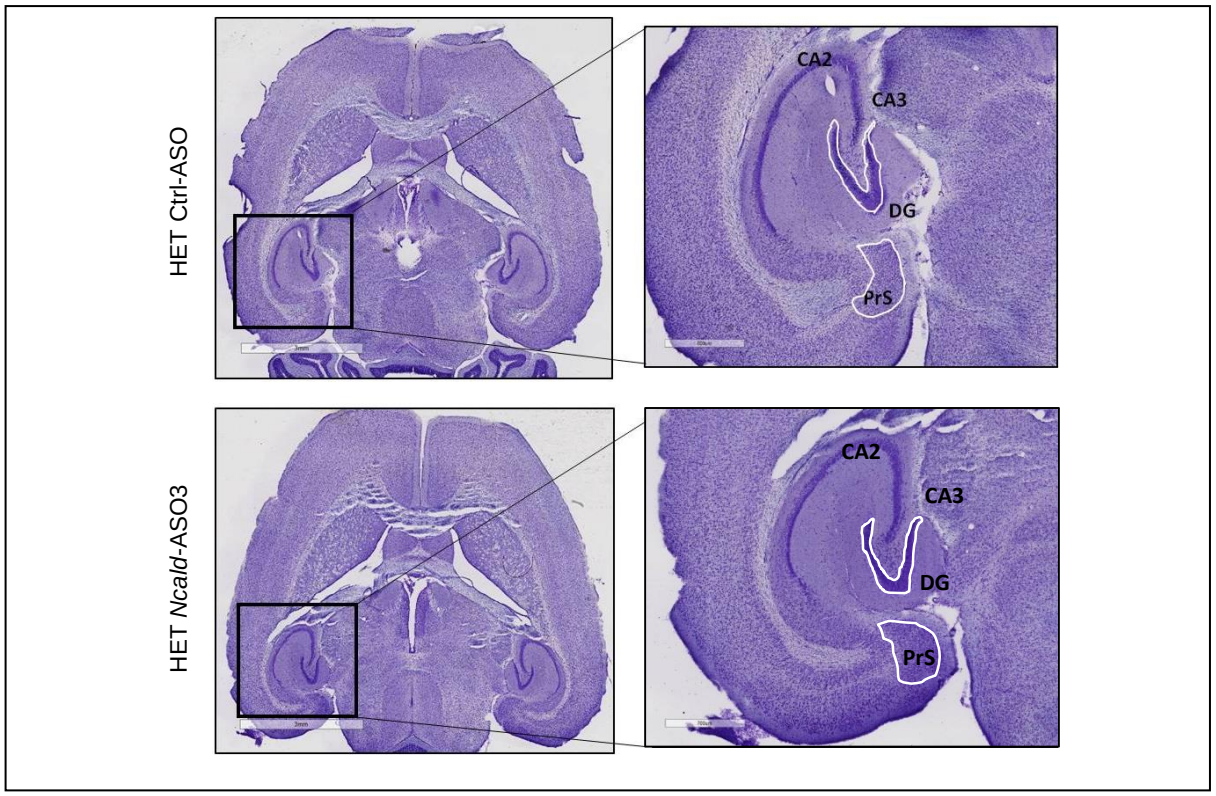

Figure S4: Brain morphology in adult mice upon *Ncald*-ASO3 treatment.

Horizontal sections of brains from 4 months **(A)** HET Ctrl-ASO and **(B)** HET *Ncald*-ASO3**.** Cresyl violet staining was performed to visualize the brain gross-morphology. CA2 and CA3, cornu ammonis hippocampal areas; DG, dentate gyrus; PrS, presubiculum. Scale bars = 100 µm.

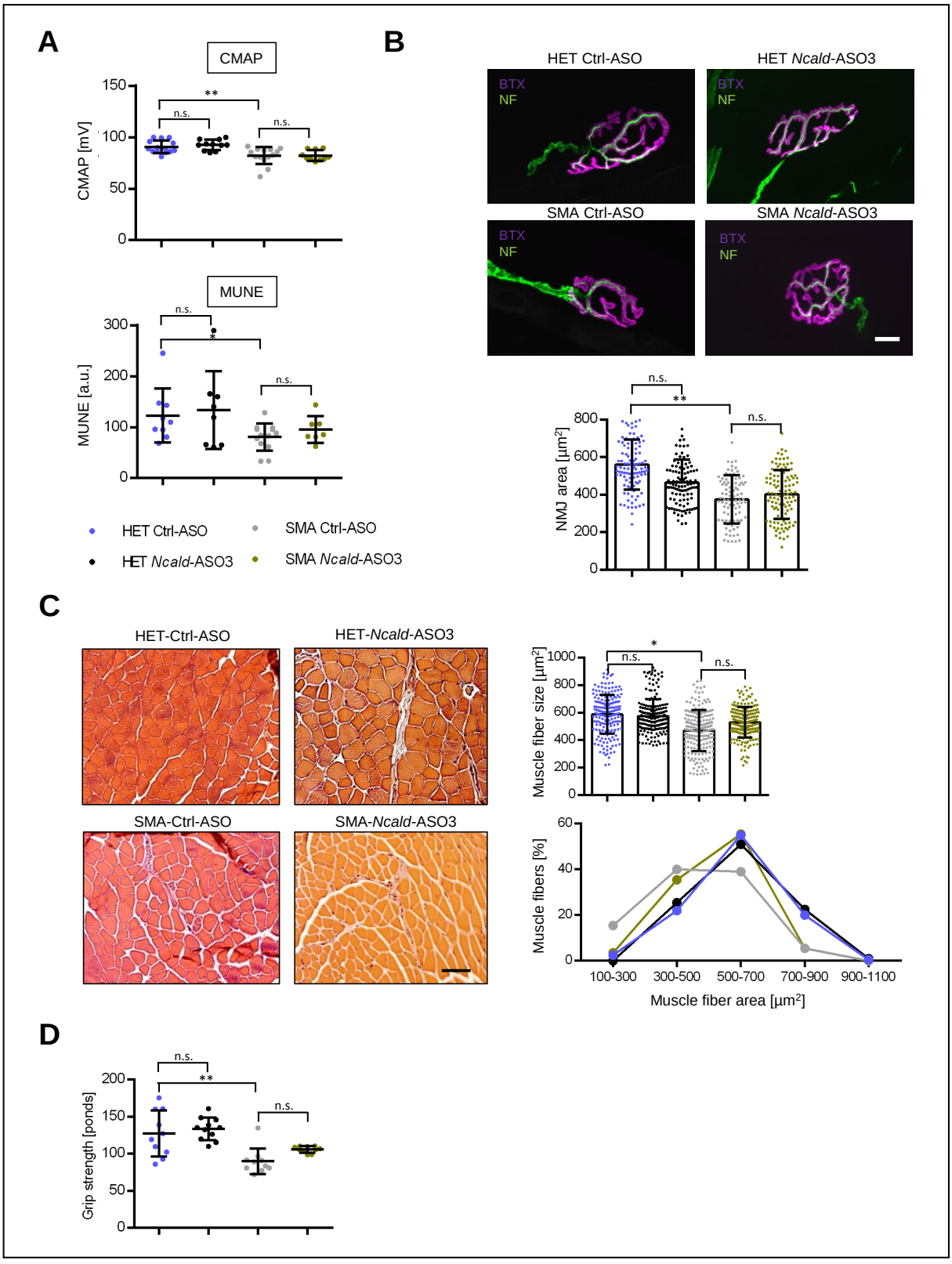

Figure S5: SMA hallmarks studied in HET and SMA animals co-injected with *SMN*-ASO and either control or *Ncald*-ASO3.

(A) Dot plot of CMAP amplitudes and MUNE values in HET and SMA animals at 3 months. Animals used for CMAP: HET Ctrl-ASO n=14; HET *Ncald*-ASO3 n=11; SMA Ctrl-ASO n=14; SMA *Ncald*-ASO3 n=10. MUNE: HET Ctrl-ASO n=9; HET *Ncald*-ASO3 n=8; SMA Ctrl-ASO n=13; SMA *Ncald*-ASO3 n=7, Color legend displayed at the bottom. For all analyses, ordinary one-way ANOVA with Tukey posthoc test for multiple comparisons was applied. n.s. = not significant, * $P < 0.05$, ** $P < 0.01$, *** $P < 0.001$

(B) Representative NMJ images in HET and SMA animals at 3 months showing postsynaptic NMJ region stained with bungarotoxin (BTX, magenta) and presynaptic nerve with neurofilament (NF; green). Graphs on the right show single dot plot values of NMJ areas of all grouped animals with mean ± SD. Quantification of maturity of NMJs with mean values of mice per group ± SD. Statistics was performed with mean values of animals per group. N = 4 animals per group, 30-55 NMJs per animal. Ordinary one-way ANOVA with Tukey posthoc test for multiple comparisons; n.s. = not significant, * $P < 0.05$, ** $P < 0.01$. Scale bars = 10 µm.

(C) Representative pictures and quantifications of haematoxylin and eosin-stained gastrocnemius (GC) muscle at 3 months. Graphs on the right show single dot plot values of GC areas of all grouped animals with mean ± SD (N = 4 animals per genotype, n = 50 fibers/mouse). For visualization, muscle fibres were grouped according to the area intervals of 100 μm^2. Ordinary one-way ANOVA with Tukey posthoc test for multiple comparisons; n.s. = not significant, * $P < 0.05$, ** $P < 0.01$. Scale bars = 50 µm.

(D) Dot plot quantification of grip strength at 6-months. Single values of each animal are shown as mean ± SD. Note that at 3 months SMA *Ncald*-ASO3 mice show stronger grip strength abilities compared to SMA Ctrl-ASO injected mice. Number of animals used are: HET Ctrl-ASO N = 10, HET *Ncald*-ASO3 N = 11, SMA Ctrl-ASO N = 10, SMA *Ncald*-ASO3 N = 10. Ordinary one-way ANOVA with Tukeys posthoc test for multiple comparisons. n.s. = not significant, * $P < 0.05$, ** $P < 0.01$, n.s. = not significant

SUPPLEMENTAL MATERIAL AND METHODS

Mouse model and genotyping

The Taiwanese SMA mice (FVB.Cg-Tg(SMN2)2Hung *Smn1*^{tm1Hung}/J, stock number 005058) were purchased from Jackson Laboratory [1]. Originally, the purchased SMA mice were on a pure FVB/N background; however, we used an additionally mouse line which has been previously backcrossed for >7 generations with C57BL6/N wildtype to obtain a pure C57BL6/N background [2]. An intermediate mouse model was produced crossing *Smn*$^{ko/ko}$*; SMN2*$^{tg/tg}$ mice on FVB background with *Smn*$^{ko/wt}$ on C57Bl6/N background to obtain both *Smn*$^{ko/wt}$*; SMN2*$^{tg/0}$ (named as HET) and *Smn*$^{ko/ko}$*; SMN2*$^{tg/0}$ (named as SMA) mixed$_{50}$ litters (50% FVB/N: 50%C57BL6/N) [3]. Primers used for litters genotyping were as follows: SmnKOfw: 50-ATAACACCACCACTCTTACTC-30; SmnKOrev1: 50-AGCCTGAAGAACGAGATCAGC-30; SmnKOrev2: 50-TAGCCGTGATGCCATTGTCA-30. A mild SMA mouse model was produced by suboptimal subcutaneous injection of severe SMA mice (50% FVB: 50% C57BL6/N) at P1 with 30 µg of SMN-ASO (Ionis Pharmaceuticals®) using a microliter syringe (Hamilton)[3].

Antisense oligonucleotides (ASOs) design

IONIS Pharmaceuticals (Carlsbad, California) designed 40 antisense oligonucleotides (ASOs) to achieve *Ncald* downregulation in the CNS. Synthesis and purification of all chemically modified oligonucleotides were performed as previously described [4]. The 5-10-5 2'-O-methoxyethyl (MOE) gapmer ASOs were 20 nucleotides in length, comprising five 2' MOE modified nucleotides on 5' and 3' wings flanking the central gap segment of ten 2'-deoxyribonucleotides. Internucleotide linkages are phosphorothioate interspersed with phosphodiester, and all cytosine residues are 5'-methylcytosines. 22 MOE gapmer ASOs targeting mouse *Ncald* efficiently suppressed *Ncald* mRNA expression in primary neuronal cultures were identified. Subsequently those 22 ASOs were tested for target reduction in the CNS of adult mice.

ASOs injection and optimization

A control-ASO (#676626) and the three *Ncald*-ASOs which achieved the highest *Ncald* KD in adult injected mice were chosen for future tolerability test: #673663 and #673672 referred to as *Ncald*-ASO1 and *Ncald*-ASO2, respectively. As those, but the control ASO showed toxicity in neonatal injected mice, we also tested the #673756 (named as *Ncald*-ASO3). Neonatal mice were i.c.v. injected in the right hemisphere close to the confluence of the sinuses with different ASOs concentration (ranging from 30 to 100 µg) [5]. All ASOs were diluted in sterile PBS and the concentration of the working solution in each case was calculated using photometric density (AD260) to administer 1.5 µl in the brain (1 µl of the ASO + 0.5 µl of 0.05% w/v trypan blue in PBS). All mice were blinded injected.

Western blot

Brain and spinal cords were dissected from experimental mice and lysed in RIPA buffer (Sigma) containing protease inhibitors (Complete Mini, Roche). Following primary antibodies were used: anti-beta-actin HRP-conjugated (A5316, Sigma), anti-SMN (mouse, MANSMA7, Hybridoma Bank; 610646, BD Biosciences), and anti-NCALD (rabbit, 12925-1-AP, Proteintech). Signal was detected with the corresponding HRP conjugated-secondary antibodies (α-mouse, Dianova, 115-035-003; α-rabbit, Cell signalling, 7074) and Chemiluminescence reagent (Thermo Scientific) according to manufacturer´s protocol.

Motoric abilities

To analyze the motoric ability of the animals, the grip strength [6] was performed with 3- and 6-month-old mice via the Grip Strength Meter (TSE System). Muscle force was recorded in pounds.

Electrophysiological biomarkers

Compound muscle action potential (CMAP) and motor unit number estimation (MUNE) were recorded to analyze motor improvement as previously described [7-9]. Mice were placed in a thermostatic warming plate at 37°C with continuous inhaled isofluorane anesthesia (1 L/min O_2 flow rate, 5% induction and 1.5-2% maintenance). Stimulation electrode was positioned in the close vicinity of the sciatic nerve and the active recording electrode was placed on the proximal gastrocnemius. UltraPro S100 from Natus Neurology components were used for the electrophysiology measurements. Nerve was stimulated with square-wave pulses of 50 μs duration and 3-10 mA amplitude to record the supramaximal response of the muscle. CMAP was expressed in mV as the peak-to-peak amplitude of the response. To estimate the motor unit number (MUNE) ten subsequent increments from the initial response were recorded and calculated according to [7]

Immunohistochemistry of NMJ

We performed the NMJ characterization and analysis in the *Transversus abdominis* muscle. Muscles from all genotypes and treated mice were dissected as previously described [10] and fixed with 4 % PFA for 20 minutes. Following primary antibodies were incubated over night at 4 °C: rabbit anti-NF-L (Cell Signalling, C28E10). Postsynaptic AChR were stained with BTX-568 (Invitrogen, B13423) which was incubated at room temperature together with secondary antibodies: rabbit AlexaFluor-488 (Invitrogen, A21206) and mouse AlexaFluor-647 (Invitrogen, A31571). Finally, muscles were mounted on slides with Prolong Gold™ antifade reagent (Invitrogen, P36934). Quantification of NMJ size and maturity was performed using ImageJ [3]. NMJ maturity was evaluated as followed: NMJs exhibiting ≥3 perforations were evaluated as mature, NMJs with <3 perforations as immature [8].

Histology

To quantify muscle fiber size on the *gastrocnemius* muscle dissection of the whole muscle was carried out. Muscles were infiltrated and embedded in paraffin and sectioned as previously described [2]. Hematoxilin (SIGMA-ALDRICH, MHS32) and eosin (ScyTek Laboratories, EYQ999) (H&E) staining was performed to visualize the fiber diameter.

For morphological analysis, a whole brain from 4-month-old HET Ctrl-ASO and HET *Ncald*-ASO3-treated mice was dissected after transcardial perfusion with 4% PFA as previously described [11]. Brain tissue and spinal cords were processed for cryocutting. Brains were cut in 10 µm slices (Cryostat, Leica). A Cresyl violet (SIGMA, C5042) staining was performed in order to visualize the brain morphology.

Image acquisition and analysis

Fluorescence images from NMJs and spinal cords were acquired with a Zeiss microscope (AxioImager.M2) supplied with the Apotome.2 system which mimics confocality. Images were acquired as Z-stacks with 40X and 63X-oil immersion objective (1.4 NA). Quantitative analysis was executed with ZEN software (Zeiss) and Fiji software. For NMJ maturity analysis, NMJs were categorized as mature with > 3 perforations and as immature with < 3 perforations. Bright field images for muscle fiber analysis were acquired with Zeiss microscope (Axioskop.2) equipped with AxioCamICc1 and 20X objective. Brain sections were imaged with Leica Slide Scanner (SCN400) and morphological analysis was executed with OMERO.insight_64. Image acquisition and analysis were performed blinded.

Statistics

Statistical analyses were performed in GraphPad Prism 6. Unpaired, two tailed Student's t-tests and one-way ANOVA statistics tests with Tukeys posthoc test for multiple comparisons were performed. Levels of statistical significance were given as follows: *$p \leq 0.05$, **$p \leq 0.01$,

and ***p ≤ 0.001. Specific tests, sample size, data representation and p-values are indicated in figure legends.

Study approval

Mice care and experiments were performed according to the institutional animal care committee guidelines and approved by LANUV NRW (Landesamt für Natur, Umwelt und Verbraucherschutz NRW) under the reference numbers 84-02.04.2014.A126.

SUPPLEMENTAL REFERENCES

1. Hsieh-Li, H.M., Chang, J.G., Jong, Y.J., Wu, M.H., Wang, N.M., Tsai, C.H., and Li, H. (2000). A mouse model for spinal muscular atrophy. Nat Genet 24, 66-70.
2. Ackermann, B., Krober, S., Torres-Benito, L., Borgmann, A., Peters, M., Hosseini Barkooie, S.M., Tejero, R., Jakubik, M., Schreml, J., Milbradt, J., et al. (2013). Plastin 3 ameliorates spinal muscular atrophy via delayed axon pruning and improves neuromuscular junction functionality. Hum Mol Genet 22, 1328-1347.
3. Riessland, M., Kaczmarek, A., Schneider, S., Swoboda, K.J., Lohr, H., Bradler, C., Grysko, V., Dimitriadi, M., Hosseinibarkooie, S., Torres-Benito, L., et al. (2017). Neurocalcin Delta Suppression Protects against Spinal Muscular Atrophy in Humans and across Species by Restoring Impaired Endocytosis. Am J Hum Genet 100, 297-315.
4. Swayze, E.E., Siwkowski, A.M., Wancewicz, E.V., Migawa, M.T., Wyrzykiewicz, T.K., Hung, G., Monia, B.P., and Bennett, C.F. (2007). Antisense oligonucleotides containing locked nucleic acid improve potency but cause significant hepatotoxicity in animals. Nucleic Acids Res 35, 687-700.
5. Glascock, J.J., Osman, E.Y., Coady, T.H., Rose, F.F., Shababi, M., and Lorson, C.L. (2011). Delivery of therapeutic agents through intracerebroventricular (ICV) and intravenous (IV) injection in mice. J Vis Exp.
6. El-Khodor, B.F., Edgar, N., Chen, A., Winberg, M.L., Joyce, C., Brunner, D., Suarez-Farinas, M., and Heyes, M.P. (2008). Identification of a battery of tests for drug candidate evaluation in the SMNDelta7 neonate model of spinal muscular atrophy. Exp Neurol 212, 29-43.
7. Arnold, W.D., Sheth, K.A., Wier, C.G., Kissel, J.T., Burghes, A.H., and Kolb, S.J. (2015). Electrophysiological Motor Unit Number Estimation (MUNE) Measuring Compound Muscle Action Potential (CMAP) in Mouse Hindlimb Muscles. J Vis Exp.
8. Bogdanik, L.P., Osborne, M.A., Davis, C., Martin, W.P., Austin, A., Rigo, F., Bennett, C.F., and Lutz, C.M. (2015). Systemic, postsymptomatic antisense oligonucleotide rescues motor unit maturation delay in a new mouse model for type II/III spinal muscular atrophy. Proc Natl Acad Sci U S A 112, E5863-5872.
9. Janzen, E., Mendoza-Ferreira, N., Hosseinibarkooie, S., Schneider, S., Hupperich, K., Tschanz, T., Grysko, V., Riessland, M., Hammerschmidt, M., Rigo, F., et al. (2018).

CHP1 reduction ameliorates spinal muscular atrophy pathology by restoring calcineurin activity and endocytosis. Brain 141, 2343-2361.

10. Torres-Benito, L., Ruiz, R., and Tabares, L. (2012). Synaptic defects in spinal muscular atrophy animal models. Dev Neurobiol 72, 126-133.

11. Upadhyay, A., Hosseinibarkooie, S., Schneider, S., Kaczmarek, A., Torres-Benito, L., Mendoza-Ferreira, N., Overhoff, M., Rombo, R., Grysko, V., Kye, M.J., et al. (2019). Neurocalcin Delta Knockout Impairs Adult Neurogenesis Whereas Half Reduction Is Not Pathological. Front Mol Neurosci 12, 19.